

Green's Function Approach to the Edge Spectral Density

J. H. Han

Department of Physics, Box 351560, University of Washington, Seattle, Washington 98195

It is shown that the conventional many-body techniques to calculate the Green's functions can be applied to the wide, compressible edge of a quantum Hall bar. The only *ansatz* we need is the existence of stable density modes that yields a simple equation of motion of the density operators. We derive the spectral density at a finite temperature and show how the tunneling characteristics of a sharp edge can be deduced as a limiting case.

PACS numbers: 73.40.Hm, 73.20.Mf

I. INTRODUCTION

Green's functions are a powerful tool for studying many-body phenomena. Since it is generally impossible to solve the many-body problem exactly, one usually relies on a set of approximation rules that will yield the calculation tractable. In one version, the difficulty is expressed in the fact that the solution of the N -particle Green's function requires the knowledge of $N + 1$ -particle function and so on *ad infinitum*. In the RPA theory of the collective oscillation,^{1,2} the density operator obeys a Heisenberg equation of motion like

$$-i\dot{\rho}(k) = [H, \rho(k)] = \omega(k)\rho(k), \quad (1.1)$$

where $\omega(k)$ is generally linear in k . Bohm and Pines¹ pointed out that Tomonaga's idea of quantizing the density operators³ are identical to their RPA theory specialized to one dimension. Much later it was realized by Everts and Schulz⁴ that, by using the above equation for the density, the Green's function hierarchy terminates at the two-particle level in one dimension, and one can solve for the single-particle spectral density exactly. They showed their results are equivalent to those previously obtained by other methods such as bosonization.⁵

The advantage of Everts' approach is that, since it is based on a more conventional technique, one can generalize it to other situations where the rigorous proof of fermion-boson equivalence may not be available. A compressible edge of the quantum Hall liquid⁶ is one such example of nearly one-dimensional systems where it is not entirely certain whether a strict bosonization theory is a valid scheme to try. Conti and Vignale⁷ and Han and Thouless⁸ have independently produced schemes general enough to accommodate the wide edge dynamics that eventually reduce to the bosonization result for the sharp edge limit. The latter approach is based on the idea of treating the density fluctuation as a hydrodynamic excitation and subsequently quantizing the classical action. The results are identical to those obtained from the independent boson model of Conti and Vignale. The validity of either approaches was not to be answered, however, unless one had a more general starting point. The Green's function approach, to be explained in this paper, provides such a starting point. It is shown that the validity of the bosonization is closely tied to the random phase approximation, namely that one has a collection of *stable* density modes obeying equations like Eq. (1.1).

The starting point of our analysis is the second-quantized Hamiltonian in the lowest Landau level. Section 2 outlines the basic formalism and derives the equation of motion for the density operator in the random phase approximation. The analysis of previous theories^{7,8} assumes the edge is an equipotential surface as the classical solution⁶ suggests. In section 3, we argue that the equipotential state is obtained as a result of the coarse-graining of the microscopic state. In section 4, it is shown how the electronic spectral properties can be derived using techniques entirely analogous to those explored by Everts and Schulz. The conventional bosonization results are recovered as a special limit. For more than one density mode present, the spectral density is a product of the spectral densities associated with the individual density mode. The electron tunneling current between two edges are derived in a closed form in section 5. The conclusion follows in section 6.

II. SECOND QUANTIZATION

Our starting point for the microscopic analysis of the edge dynamics is the Hamiltonian

$$H = \frac{e^2}{2\kappa} \int \frac{1}{|r - r'|} \psi^\dagger(r) \psi^\dagger(r') \psi(r') \psi(r) d^2r d^2r' + \int V_i(r) \psi^\dagger(r) \psi(r) d^2r. \quad (2.1)$$

which consists of the Coulomb interaction and the external potential. There is no kinetic energy term as we are working exclusively within the lowest Landau level. We can write out the various operators in the basis of wavefunctions in the lowest Landau level. We will use L for the length (perimeter) of the Hall bar (droplet).

$$\psi(r) = \pi^{-1/4} L^{-1/2} \sum_k e^{ikx} e^{-\frac{1}{2}(y-k)^2} c_k. \quad (2.2)$$

When this expression is substituted in the Hamiltonian, Eq. (2.1), we obtain the second-quantized version of the Hamiltonian in momentum space

$$\begin{aligned} H &= H_C + H_i, \\ H_C &= \frac{1}{2} \sum_{k_1 k_2 q} V_C(q, k_1 - k_2) c_{k_1+q/2}^\dagger c_{k_2-q/2}^\dagger c_{k_2+q/2} c_{k_1-q/2}, \\ H_i &= \sum_{kq} V_i(q, k) c_{k+q/2}^\dagger c_{k-q/2}. \end{aligned} \quad (2.3)$$

We have used the electronic basis to expand the Hamiltonian, and consequently our theory may be more suitable to describe the integer edge. There is no known way one can arrive at something like a Laughlin state from the above type of Hamiltonian and working one's way up through diagrammatic theory. With the wide edge, our theory may still be valid a sufficient distance away from the fractional bulk where fractional quasiparticle states are unlikely to exist, but is less certain to work close to the bulk where a small decrease in density from the bulk value may be better described as a dilute set of quasiholes. We will adopt the above Hamiltonian as a starting point, if for lack of a better one, and see if something sensible can come out of it. Quite surprisingly, the electronic properties of the fractional edge such as spectral density and the electron tunneling current follow very straightforwardly from the above Hamiltonian.

The definition of the Coulomb and the external potential in the momentum representation are the following:

$$\begin{aligned} V_C(q, k) &= \frac{2e^2}{\sqrt{2\pi\kappa L}} e^{-q^2/2} \int_{-\infty}^{\infty} dy K_0(|qk+qy|) e^{-y^2/2}, \\ V_i(q, k) &= \frac{1}{\sqrt{\pi L}} e^{-q^2/4} \int V_i(x, y) e^{-iqx-(y-k)^2} dx dy. \end{aligned} \quad (2.4)$$

The kernel is the modified Bessel function K_0 . For the external potential which depends on y only, we obtain a simpler expression,

$$V_i(k) = V_i(0, k) = \pi^{-1/2} \int V_i(y) e^{-(y-k)^2} dy. \quad (2.5)$$

The confining potential of a Hall bar with the translation symmetry in the x direction would be such a case. In this paper, we will restrict ourselves to this form of the external potential.

Note that the integral for $V_C(q, k)$ is the convolution of the modified Bessel function with a gaussian of width l_0 , which we have taken to be unity. For the limit of a very strong magnetic field, the integral is approximately equal to $\sqrt{2\pi} K_0(|qk|)$. In the classical treatment of Aleiner and Glazman⁹, the kernel was simply this modified Bessel function. The classical theory does not explicitly take the size of the electron wavefunction into account which in our case is the magnetic length. When we do, it turns out the relevant quantities are the convolution of the classical quantities with an envelope function of the width of the magnetic length as evidenced in Eq. (2.4). For clarity, we have plotted $V(q, k)$ and $\sqrt{2\pi} K_0(|qk|)$ for $q = 10^{-2}$ in Fig. 1. The difference is minute in almost all regions of k except very close to the origin. At $k = 0$, the classical kernel diverges logarithmically, while $V_C(q, 0) = (e^2/\kappa L) e^{-q^2/4} K_0(q^2/4)$ leading to a finite interaction energy even at zero distance.

We will work out the time development of $c_{k+q/2}^\dagger c_{k-q/2}$, since it is this type of operator that gives rise to the density fluctuation. The commutator with the Coulomb part of the Hamiltonian gives

$$\begin{aligned} [H_C, c_{k+q/2}^\dagger c_{k-q/2}] &= \sum_{pk'} V_C(p, k-k'+\frac{1}{2}(q+p)) c_{k+p+q/2}^\dagger c_{k'-p/2}^\dagger c_{k'+p/2} c_{k-p-q/2} \\ &\quad - \sum_{pk'} V_C(p, k-k'-\frac{1}{2}(q+p)) c_{k+q/2}^\dagger c_{k'-p/2}^\dagger c_{k'+p/2} c_{k-p-q/2}. \end{aligned} \quad (2.6)$$

We are confronted with a generally intractable equation, with all possible momentum-preserving processes contributing to the equation of motion with a certain matrix element. In the RPA theory², the four-point operator $c^\dagger c^\dagger cc$ is replaced by the contraction of one of the $c^\dagger c$ pairs multiplied by an operator of the form $c_{k'+q}^\dagger c_{k'}$. The contraction gives zero from translation invariance unless the momentum indices are the same, in which case we get $c_{k'}^\dagger c_{k'} \rightarrow n_{k'}$, the electron occupation for a given quantum number k' . There are four ways of pairing one creation and one annihilation operator in $c^\dagger c^\dagger cc$. In a recent numerical study¹⁰, it was argued that the ground state of the edge is in fact not translation-invariant but a kind of spontaneously broken symmetry state with charge modulation along the symmetry direction. For such a system, $\langle c_k^\dagger c_{k'} \rangle$ is nonzero even for $k \neq k'$. Detailed discussion of the symmetry breaking state is not pursued here.

When we put all the terms in the RPA together,

$$\begin{aligned} [H_C, c_{k+q/2}^\dagger c_{k-q/2}]_{\text{RPA}} &= (n_{k-q/2} - n_{k+q/2}) \sum_{k'} [V_C(q, k-k') - V_C(k-k', q)] c_{k'+q/2}^\dagger c_{k'-q/2} \\ &+ c_{k+q/2}^\dagger c_{k-q/2} \sum_{k'} [V_C(0, k-k') - V_C(k-k', 0)] (n_{k'+q/2} - n_{k'-q/2}). \end{aligned} \quad (2.7)$$

The commutator with the external potential gives

$$[H_i, c_{k+q/2}^\dagger c_{k-q/2}] = [V_i(k+q/2) - V_i(k-q/2)] c_{k+q/2}^\dagger c_{k-q/2}. \quad (2.8)$$

The significance of Eqs. (2.7) and (2.8) can be quite easily seen if we first define the Hartree-Fock potential and the local energy $E(k)$ as

$$V_{HF}(q, k-k') = V_C(q, k-k') - V_C(k-k', q), \quad (2.9)$$

$$E(k) = V_i(k) + \sum_{k'} V_{HF}(0, k-k') n_{k'}. \quad (2.10)$$

The net equation of motion looks very simple:

$$\begin{aligned} [H, c_{k+q/2}^\dagger c_{k-q/2}] &= (n_{k-q/2} - n_{k+q/2}) \sum_{k'} V_{HF}(q, k-k') c_{k'+q/2}^\dagger c_{k'-q/2} \\ &+ [E(k+q/2) - E(k-q/2)] c_{k+q/2}^\dagger c_{k-q/2}. \end{aligned} \quad (2.11)$$

The first line may be interpreted as the local density fluctuation centered at k interacting via the Hartree-Fock potential $V_{HF}(q, k-k')$ with the density fluctuation at another point k' . The single-particle energy term $E(k)$ turns out to be the convolution of the total static energy (external+Coulomb) at y with $e^{-(y-k)^2}$. The static Coulomb energy also includes the exchange contribution.

For a translationally invariant two-dimensional electron gas, the Hartree and the Fock terms will be proportional to $1/q$ and $1/|\vec{k}-\vec{k}'|$ respectively. In the basis of the Landau wavefunctions we adopted here, the Hartree term no longer depends exclusively on the transferred momentum q . From the definition of the Hartree-Fock potential in Eq. (2.9), one can see that the Hartree and the Fock terms are related by the interchange of the two arguments in $V_C(q, k)$. In our particular representation, the Hartree-Fock term may be understood as simply a Hartree potential with reduced strength. Examination of Eq. (2.9) shows that $V_{HF}(q, k)$ becomes negative for the separation $k < q$.

Proper treatment of the dynamics in Eq. (2.11) requires first the understanding of the ground state configuration, $\{n_k\}$. At zero temperature, the occupation is either zero or one. The minimization of the energy functional

$$E[\{n_k\}] = \sum_k V_i(k) n_k + \frac{1}{2} \sum_{k, k'} V_{HF}(0, k-k') n_k n_{k'} \quad (2.12)$$

determines the distribution $\{n_k\}$. A thorough discussion of the ground state is quite subtle and will be relegated to the next section. If we allowed the n_k to vary continuously between 0 and 1, the variation of the above functional is straightforward, and the minimum is given by¹¹

$$E(k) = V_i(k) + \sum_{k'} V_{HF}(0, k-k') n_{k'} = \text{constant}. \quad (2.13)$$

The ground state would be given by the screened state for which $E(k)$ is uniform everywhere. One can argue, as we will in the next section, that by the coarse-graining of the microscopic configuration one does have a smooth variation

in n_k and the uniform energy $E(k)$ in the ground state. In that case, the single-particle term in Eq. (2.11) disappears and the solution for the particle-hole dynamics is given in the form

$$\begin{aligned}\rho_\alpha(q) &= \sum_k h_\alpha(k) (c_{k+q/2}^\dagger c_{k-q/2} - \delta_{q0} n_k), \\ [H, \rho_\alpha(q)] &= \omega_\alpha(q) \rho_\alpha(q).\end{aligned}\tag{2.14}$$

For the smooth and monotone occupation, we can replace $n_{k-q/2} - n_{k+q/2}$ by its gradient, and $h_\alpha(k)$ becomes the analogue of the classical eigenfunction.⁷⁻⁹ The discrete matrix equation satisfied by $h_\alpha(k)$ is

$$\sum_{k'} V_{HF}(q, k-k') [n_{k'-q/2} - n_{k'+q/2}] h_\alpha(k') = \omega_\alpha(q) h_\alpha(k).\tag{2.15}$$

In principle the eigenfunctions also depend on q , but the dependence is very weak at small q .¹² We will therefore omit the q dependence in our definition of $h_\alpha(k)$. Take $h_\alpha(k)$ to be the eigenfunction in the presence of the Hartree term alone, then using the first-order perturbation theory, the relative correction in the phase velocity $v_\alpha(q) = \omega_\alpha(q)/q$ due to the Fock term is

$$\frac{\delta v_\alpha(q)}{v_\alpha(q)} = - \frac{\iint h_\alpha(k) V_C(k-k', q) h_\alpha(k') d n_k d n_{k'}}{\iint h_\alpha(k) V_C(q, k-k') h_\alpha(k') d n_k d n_{k'}}.\tag{2.16}$$

The Fock term extends over the distance of the magnetic length, $|k - k'| \leq l_0$ while the Hartree term is not limited by any such cutoff except the width of the edge, a . From dimensional analysis alone, one can see that the above term is of order l_0/a which is very small for a compressible edge. The influence of the Fock term on the dynamics is consequently small.

Because of the symmetry of the kernel $V_{HF}(q, k - k')$ under the interchange $k \leftrightarrow k'$ and $q \rightarrow -q$, one can write it out in terms of the complete set of eigenfunctions $h_\alpha(k)$ as^{8,13}

$$V(q, k-k') = \frac{2\pi^2}{\nu L} \sum_{\alpha=0}^{\infty} v_\alpha(q) h_\alpha(k) h_\alpha(k').\tag{2.17}$$

This way of writing out the kernel will prove useful for the subsequent analysis.

The time evolution of the single-particle operator c_p is given by

$$\begin{aligned}[H, c_p] &= \sum_{kq} V_C(q, k-p-q/2) c_{k+q/2}^\dagger c_{p+q} c_{k-q/2} - V_i(p) c_p \\ &= -E(p) c_p - \frac{2\pi^2}{\nu L} \sum_{\alpha, q \neq 0} v_\alpha(q) h_\alpha(p+q/2) \rho_\alpha(q) c_{p+q}.\end{aligned}\tag{2.18}$$

The energy term $E(p)$ is obtained from contraction of the operators $c^\dagger c c$. We have used the Eq. (2.17) to expand the potential term in terms of the constituent density modes. Unlike the time evolution of the density operators, we have kept the scattering terms in the commutator, giving rise to the coupling between a single-particle operator and a density operator $\rho_\alpha(q)$. The sum is restricted to $q \neq 0$ to guarantee c_{p+q} does not coincide with c_p . All the diagonal contributions are contained in $E(p)$. All the dynamics of the system within our RPA framework is contained in Eqs. (2.11) and (2.18).

III. EDGE RECONSTRUCTION

For a very long Hall bar with the electrons occupying the bulk with uniform density, the electric field generated by the charges diverges logarithmically as one approaches the edge. Quantum-mechanically the divergence is cancelled by the exchange potential, with the result that the field remains finite and proportional to the logarithm of the width $2W$ of the bar. The confining potential is required to compensate for this outward force if the charge configuration is to remain stable. It is easy to estimate what the critical field is if we use the harmonic confining potential given by

$$V_i(k) = \frac{1}{2} \alpha k^2.\tag{3.1}$$

The Hartree and Fock energies can be calculated for the electron occupation $n_k = \theta(W - |k|)$. The force exerted at position k due to the electrons is

$$-\frac{\partial E_{HF}(k)}{\partial k} = \frac{e^2}{2\pi\kappa} [2 \ln \left(\frac{1+x}{1-x} \right) + e^{-W^2(1+x)^2/4} K_0(W^2(1+x)^2/4) - e^{-W^2(1-x)^2/4} K_0(W^2(1-x)^2/4)]. \quad (3.2)$$

The logarithmic part comes from the Hartree interaction. Close to the edge $x = k/W \approx \pm 1$, one of the modified Bessel functions diverges logarithmically and cancels the divergence of the Hartree force, leaving the field strength at $(e^2/2\pi\kappa) \ln(W^2 e^\gamma/2)$. The stability is achieved if the confining field strength at the edge is greater than the repulsive force of the Hartree-Fock potential:

$$\alpha W \geq \frac{e^2}{2\pi\kappa} \ln(W^2 e^\gamma/2). \quad (3.3)$$

For a sufficiently narrow bar or a weak enough confining potential this condition is violated, and a certain amount of charges separate away from the bulk. This newly formed “island” experiences a stronger confining field, but it cannot merge with the bulk from which it got separated because of the repulsive Hartree-Fock force. As a result, the center of the new island will sit at some equilibrium position away from the bulk. Approximately, the position of the center will be

$$W + \delta W = \frac{e^2}{2\pi\kappa\alpha} \ln \frac{W^2 e^\gamma}{2}. \quad (3.4)$$

Because the condition Eq. (3.3) is violated in order for the islands to form, the right hand side is slightly greater than W .

The fate of the newly formed island will be subject to the same stability criteria as Eq. (3.3) with the difference that, in place of the bare confining potential, we now use the effective potential composed of $V_i(k)$ and the interaction potential with the “parent” island. If the new island does not satisfy the stability criteria, it will further split into smaller islands until the stability is obtained. By continuing to lower the bare potential parameter α , one should expect this “reconstruction”¹⁴ process to repeat itself over many times.

So how is it possible that we recover the classical density profile $n(x)$ from an apparently discrete and discontinuous distribution of electrons? First think of the following correspondence between real and momentum space distribution:

$$n(x) = A \sum_{k=i\Delta} n_k e^{-(x-k)^2}. \quad (3.5)$$

The momentum space distribution function is taken to be the value of the known real space density $n(x)$ (hence continuous) at a given site, $n_k = n(x = i\Delta)$ (i =integer), where Δ is the sampling step. The overall normalization on the r.h.s. is fixed by A . Take, for example, the density used by Aleiner and Glazman⁹; $n(x) = \arctan \sqrt{x/a}$. Can we pick a mesh size Δ so that the sum in Eq. (3.5) reproduces the real space density? Considering that the gaussian has a width of unity, it is expected that Δ ought to be comparable or less than unity. As it turns out, using $\Delta = 1$ already gives an adequate reproduction of $n(x)$ over an entire region of space except very close to the edge (Fig. 2). Because of the finite extent of the gaussian, the density does not cut off where the classical density normally does.

The spacing between electron states is $2\pi/L$. For a Hall bar of length 1mm, one magnetic length width is large enough to contain

$$N_c = \frac{L}{2\pi l_0} \approx 10^4 \quad (3.6)$$

states. The microscopic ground state for a very smooth confining potential is one in which there are a large number of islands, of varying sizes and varying separations between the neighbors, with the center of each island positioned at the local self-consistent potential minimum. Provided the reconstruction has reduced the size of the individual island to a sufficiently small fraction of the magnetic length, one expects the coarse graining of occupation to give rise to the smooth average occupation, which in turn closely follows the classical density profile. An illustration of this point is given in Fig. 3. Here we have chosen a configuration of islands that approximate the real-space density of the electrostatic solution, $n(x) = \arctan(x/a)^{1/2}$. The underlying occupation n_k is non-monotonic, but the density itself is a monotone increasing function. As figure 2 suggests, the averaged occupation n_k will follow the density $n(x)$ and hence also monotone. One can go back to Eq. (2.12) and treat n_k as an averaged, continuous quantity. The screened state of the classical electrostatics follows as a consequence.

The choice of the island configuration for figure 3 is arbitrary, and does not represent the energy-minimizing state. A detailed numerical study in the future is needed to understand the island distribution from the proper energetic consideration. The arguments of the preceding paragraph suggests, we believe, a plausible scenario which also attempts to link the Hartree-Fock theory (reconstruction picture) with the classical picture of monotone density.

The dynamical correspondence between the Hartree-Fock and the classical theories can be similarly established. A given island is subject to two types of excitations. First is the harmonic motion of its center of mass about the local minimum. Alternatively it can create a density fluctuation at either edges. As Chamon and Wen¹⁴ showed, the latter type of excitation does not propagate very far, because even a small amount of impurities (backscattering) in the substrate will be sufficient to localize the excitation. For $N - 1$ islands present, there are thus N dynamical degrees of freedom, since we have to include the density fluctuations at the boundary of the parent island as well as the center coordinate of each island. A coherent motion of all the center-of-mass coordinates would correspond to the EMP mode. All other modes will become the $N - 1$ acoustic modes, where some of the islands move out of phase with the rest.^{10,15} In the classical theory, there was no limit on the number of acoustic modes present. The present microscopic picture suggests that the upper limit on the possible modes is the number of islands that make up the edge. Further effects such as damping will reduce the number of surviving modes.

The argument presented in this section is valid for integer edge states without the extra correlation energy associated with the fractional bulk. For fractional edge states, Hartree-Fock theory of composite fermions had been considered.¹⁶ The situation is more complicated with composite fermions because, in addition to the interplay of the confining and the Coulomb potentials, one also has to put the correlation energy into play. For integer states, an arbitrary smooth confining potential will lead to an arbitrary small island. In the fractional case, the correlation energy may overcome the Coulomb repulsion and resist further splitting even for a very weak confinement. The size of such an island may not be small enough to validly apply the coarse-graining scheme. Consideration of such cases is clearly outside the scope of the present paper. We will treat the edge as a set of microscopically large but macroscopically small islands whose coarse-graining will reproduce the classical picture of screening. It should also be noted that Franco's calculation¹⁰ actually yields the screened state as a ground state without any coarse-graining. A thermal averaging of low-lying energy configurations will also yield a picture similar to the coarse-graining.

IV. GREEN'S FUNCTIONS

With this background, it is now possible to calculate the Green's functions. Define the one- and two-particle functions as

$$\begin{aligned} G_p(t) &= -i\langle T c_p(t) c_p^\dagger(0) \rangle, \\ B_\alpha(q, t; p+q, t') &= \langle T \rho_\alpha(q, t) c_{p+q}(t') c_p^\dagger(0) \rangle. \end{aligned} \quad (4.1)$$

with $\rho_\alpha(q)$ defined as in Eq. (2.14). The average $\langle \dots \rangle$ is over all many-body states with the Boltzmann weight $e^{-\beta E}$ for each state. After a straightforward algebra, one has

$$\begin{aligned} \frac{\partial G_p(t)}{\partial t} &= -i\delta(t) - \frac{2\pi^2}{\nu L} \sum_{\alpha, q} v_\alpha(q) h_\alpha(p+q/2) B_\alpha(q, t; p+q, t^-), \\ \left\{ \frac{\partial}{\partial t} + i\omega_\alpha(q) \right\} B_\alpha(q, t; p+q, t') &= i h_\alpha(p+q/2) \{ \delta(t) G_{p+q}(t') - \delta(t - t') G_p(t) \}. \end{aligned} \quad (4.2)$$

In arriving at the above result, we have used Eqs. (2.11) and (2.18). The sum over the density modes in the first half of the Eq. (4.2) is a result of rewriting the potential in terms of the eigenfunctions as in Eq. (2.17). The single-particle energy $E(p)$ is taken to be uniform and set to zero for all p after coarse-graining. We have used the full equation of motion for c_p , and the approximate RPA equation for the density. In effect, RPA truncates the Green's function hierarchy at the two-particle level and we have a closed set of equations to solve. The symbol t^- indicates that the time for the operator c_{p+q} in the Eq. (4.1) is supposed to be taken infinitesimally earlier than for $\rho_\alpha(q)$.

One can remove $B_\alpha(q, t; p+q, t')$ from the above equations. We adopt the Matsubara representation and write

$$i\omega G_p(i\omega) = -1 + \frac{2\pi^2}{\beta\nu L} \sum_{\alpha q \Omega} v_\alpha(q) h_\alpha^2(p+q/2) \frac{G_{p+q}(i\omega + i\Omega) - G_p(i\omega)}{i\Omega - \omega_\alpha(q)}. \quad (4.3)$$

The sum over q and Ω runs from minus to plus infinity as multiples of $2\pi/L$ and $2\pi/\beta$ respectively. The argument ω is an odd multiple of π/β since it enters in the fermionic Green's function. It then follows that Ω should be an even multiple of π/β . The thermal sum \sum_{Ω} can be evaluated with standard techniques¹⁷

$$\begin{aligned} \frac{1}{\beta} \sum_{\Omega} \frac{G_{p+q}(i\omega + i\Omega)}{i\Omega - \omega_{\alpha}} &= \int_{-\infty}^{\infty} \frac{dx}{1+e^{\beta x}} \frac{A_{p+q}(x)}{x - i\omega - \omega_{\alpha}} - B(\omega_{\alpha})G_{p+q}(i\omega + \omega_{\alpha}), \\ \frac{1}{\beta} \sum_{\Omega} \frac{1}{i\Omega - \omega_{\alpha}} &= \frac{-1/2}{\tanh \beta \omega_{\alpha}/2}. \end{aligned} \quad (4.4)$$

We have introduced the Bose distribution function $B(x) \equiv (e^{\beta x} - 1)^{-1}$ above. The Fermi function will be similarly defined as $F(x) = (e^{\beta x} + 1)^{-1}$.

One can now revert to real frequencies $i\omega \rightarrow \omega \pm i0$ and take the difference $G_p(\omega + i0) - G_p(\omega - i0) \equiv -2\pi i A_p(\omega)$, which is the spectral density. The spectral density obeys the equation

$$\begin{aligned} \omega A_p(\omega) &= -\frac{2\pi^2}{\nu L} \sum_{\alpha q} v_{\alpha}(q) h_{\alpha}^2(p+q/2) \{F(\omega + \omega_{\alpha}) + B(\omega_{\alpha})\} A_{p+q}(\omega + \omega_{\alpha}) \\ &\quad + \frac{\pi^2}{\nu L} \sum_{\alpha q} v_{\alpha}(q) h_{\alpha}^2(p+q/2) \frac{A_p(\omega)}{\tanh \beta \omega_{\alpha}/2}. \end{aligned} \quad (4.5)$$

The above equation is rather complicated, and it is hard to believe one can solve for the spectral density in this form. The reason for the difficulty is that Eq. (4.5) couples the spectral densities at different p 's. A great simplification can be achieved if we assume that we can ignore such a coupling:

$$\begin{aligned} A_{p+q}(\omega) &\rightarrow A_p(\omega), \\ h_{\alpha}(p+q/2) &\rightarrow h_{\alpha}(p). \end{aligned} \quad (4.6)$$

With this simplification the last term in Eq. (4.5) disappears from symmetry, and we have the following simplified equation for $A_p(\omega)$:

$$\omega A_p(\omega) = -\frac{2\pi^2}{\nu L} \sum_{\alpha q} v_{\alpha}(q) h_{\alpha}^2(p) \{F(\omega + \omega_{\alpha}) + B(\omega_{\alpha})\} A_p(\omega + \omega_{\alpha}). \quad (4.7)$$

We have not attempted to justify the above simplification except on the ground that we are keeping the lowest order terms in what may be considered an expansion in small q .

Consider first the zero temperature limit of the above result. The distribution functions reduce to step functions; $F(x) = \theta(-x)$, $B(x) = -\theta(-x)$. The sum of Fermi and Bose functions survives only in the range $-\omega < \omega_{\alpha} < 0$, and Eq. (4.7) turns into

$$\omega A_p(\omega) = \frac{2\pi^2}{\nu L} \sum_q \sum_{\alpha} v_{\alpha}(q) h_{\alpha}^2(p) A_p(\omega + \omega_{\alpha}). \quad (4.8)$$

The sum over q is restricted to the range $-\omega < \omega_{\alpha}(q) < 0$ for each α . The q -dependence of the velocity $v_{\alpha}(q)$ is logarithmic if it is the EMP mode, and nearly constant for the acoustic ones. One can fix the q entering in the velocities with some momentum or the (inverse) length scale associated with the particular problem at hand. Since the dependence is logarithmic, it should not matter which scale we choose to fix q . Treating all v_{α} 's as constants, we recover the relation first derived by Conti and Vignale⁷

$$\omega A_p(\omega) = \sum_{\alpha} \frac{\pi}{\nu} h_{\alpha}^2(p) \times \int_0^{\omega} A_p(\omega') d\omega'. \quad (4.9)$$

The solution is a power-law $A_p(\omega) \propto \omega^{\kappa_p - 1}$ with the exponent

$$\kappa_p = \sum_{\alpha} \frac{\pi}{\nu} h_{\alpha}^2(p). \quad (4.10)$$

This is the same tunneling exponent derived previously^{7,8} and is given by the sum of the exponents associated with each density mode. The Green's function approach, rather than contradicting any of the previous theories, serves to clarify what physical and mathematical approximations were involved in previous theories.

At a non-zero temperature, we follow the method explored by Everts and Schulz⁴ and write $A_p(\omega) = F(\omega)^{-1} A'_p(\omega)$:

$$\omega A'_p(\omega) = \kappa_p \int_{-\infty}^{\infty} d\omega B(\omega) A'_p(\Omega - \omega). \quad (4.11)$$

It requires a series of mathematical manipulations to solve this equation, and details can be found in the appendix. We will proceed to the final result for the spectral density:

$$A_p(\omega) = T^{\kappa_p-1} \cosh\left(\frac{\beta\omega}{2}\right) \Gamma\left(\frac{\kappa_p}{2} + \frac{i\beta\omega}{2\pi}\right) \Gamma\left(\frac{\kappa_p}{2} - \frac{i\beta\omega}{2\pi}\right). \quad (4.12)$$

It is a position-dependent spectral density since κ_p varies with p . The tunneling exponent is significantly larger for a compressible edge with a large number of modes, since κ_p is proportional to the squares of the eigenfunctions. For a sharp edge, there are no reconstructed islands, and it is only the edge of the bulk that fluctuates. The corresponding eigenfunction is a structureless constant which, after normalization, becomes $1/\sqrt{\pi}$. When substituted, κ equals $1/\nu$ independent of p . This is precisely the result one obtains from bosonization.

For principal fractions ($\nu = 1/m$), the spectral densities can be calculated in closed forms. Writing $A_m(\omega)$ as the spectral density of the fraction $1/m$, one can deduce from Eq. (4.12) the recursion relation

$$A_{m+2}(\omega) = [\omega^2 + (\pi m T)^2] A_m(\omega) \quad (4.13)$$

up to the proportionality factor. Since $A_1(\omega) = 1$, $A_2(\omega) = \omega / \tanh(\beta\omega/2)$, we can calculate the spectral densities associated with arbitrary fractions $1/m$. Generally, the spectral density has an asymptotic limit ω^{m-1} and T^{m-1} for high and low ratios of ω/T respectively. The even denominators have the $\coth(\beta\omega/2)$ factor associated in their spectral densities while it is a polynomial for the odd denominators.

V. TUNNELING CURRENTS

One can imagine the edges of the two quantum Hall liquids brought in sufficient proximity to allow tunneling between point p on one edge and p' on the other. The impurity charge is assumed to mediate the scattering between edges. Also by locally changing the gate voltage, one can induce a finite curvature in the edge shape which results in the loss of translation symmetry and therefore, a finite amplitude for tunneling. We will consider a single scattering process (Fermi's Golden Rule) with a fixed, constant scattering matrix element. The electron tunneling current between the edges is proportional to the integral

$$\int_{-\infty}^{\infty} A_{\kappa_p}(\omega - V/2) A_{\kappa_{p'}}(\omega + V/2) \times \{F(\omega + V/2) - F(\omega - V/2)\} d\omega. \quad (5.1)$$

where V is the chemical potential difference of the two edges. For the tunneling current at a finite temperature, one needs to use the expression of the spectral density in Eq. (4.12). The tunneling current characterized by two tunneling exponents $(\kappa_p, \kappa_{p'})$ turns out to be ($\kappa = \kappa_p + \kappa_{p'}$)

$$I_{\kappa}(V) = T^{\kappa-1} \sinh\left(\frac{\beta V}{2}\right) \Gamma\left(\frac{\kappa}{2} + i\frac{\beta V}{2\pi}\right) \Gamma\left(\frac{\kappa}{2} - i\frac{\beta V}{2\pi}\right). \quad (5.2)$$

As it happens, the tunneling current is only dependent on the sum of the tunneling exponents. Compare this expression with that for the spectral density, Eq. (4.12), and one finds they are very similar. The recursion relation for the current will be the same as derived in Eq. (4.13). We need to know the $I_1(V)$ and $I_2(V)$ to derive the tunneling current for all integer values of κ .

$$I_1(V) = \tanh\left(\frac{\beta V}{2}\right), \quad I_2(V) = V. \quad (5.3)$$

We can specialize to the limit of a sharp edge, where the significance κ is the sum of the two inverse fractions for each edge; $\kappa = m + n$. The tunneling formula in this case has been derived by Wen¹⁸ and agrees with our result. One sees that, for example, a tunneling between $\nu = 1$ and $\nu = 1/3$ edge ($\kappa = 4$) would give the same $I(V)$ curve as tunneling between two $1/2$ edges. The same is true of two $1/3$ edges and 1 and $1/5$. This symmetry is inherent in the chiral Luttinger liquid action¹⁹ and is explicitly demonstrated in the above calculation. In the zero temperature limit, I_{κ} is proportional to $V^{\kappa-1}$. For a high enough temperature we are back in the ohmic regime with the conductance proportional to $T^{\kappa-2}$. The crossover between the two regimes occurs around $T/V \equiv 1$.

VI. CONCLUSION

We have demonstrated that all the electronic spectral properties of the quantum Hall edges, both wide and sharp, can be derived by using the equation of motion method and the conventional many-body theory. We relate the bosonization theory of the edge state to the random phase approximation and argue that they are in fact equivalent. It may happen that the real system is subject to a rather large dissipation, or that the terms neglected in the random phase approximation actually contribute significantly. These possibilities and their consequences on tunneling are not understood in detail. One can, however, rather easily see the consequence of a stable density mode whose dispersion is not linear with q but goes as q^η where η may be an arbitrary positive number. Going back to Eq. (4.8), it can be shown that a single-mode edge at zero temperature with the tunneling exponent κ and the collective dispersion exponent η obeys

$$\omega A(\omega) = \frac{\kappa}{\eta} \int_0^\omega A(\omega') d\omega'. \quad (6.1)$$

The actual tunneling exponent is κ/η . The suppression of the low-lying excitations leads to the *enhanced* tunneling at low energy. It is therefore crucial in the determination of the tunneling exponent that we know the precise power-law dependence of the dispersion as well. We have been somewhat cavalier about taking the results of our calculation to both the odd and even fractions, while there is a marked difference in the bulk properties of the even and odd denominator states. It is still true there are gapless modes close to the edge for any fractions. For the gapless, even-denominator states the edge excitation will couple to the bulk fluctuation, possibly changing the dispersion relation to deviate from linearity. Our formula in Eq. (6.1) suggests that the spectral density will behave as $\omega^{m/\eta-1}$ for a filling fraction $1/m$ whose gapless mode has a dispersion like $\omega(q) \propto q^\eta$. Presence of several gapless modes will contribute independently to the exponent in the usual manner.

We have used the electronic basis to expand the second-quantized Hamiltonian and consequently, we are not able to discuss the fractionally-charged quasiparticles within the current framework. Tunneling experiments between the chiral edges through the fractional bulk²⁰ is outside the scope of the theory presented in this paper. For this purpose, one must still rely on the effective theories.^{8,21} For the recent experiment of *electron* tunneling to the edge of the fractional liquid,²² our result gives a good fit to the observed I-V curve.

The author wishes to acknowledge helpful conversations with Albert Chang, Michael Geller, Matt Grayson, David Thouless and Carlos Wexler. This work was supported by an NSF grant, DMR-9628345.

APPENDIX: EVALUATING THE SPECTRAL DENSITY AT A FINITE TEMPERATURE

One wants to solve the Eq. (4.11),

$$\begin{aligned} \omega A'_p(\omega) &= \kappa_p \int_{-\infty}^{\infty} d\omega B(\omega) A'_p(\Omega - \omega), \\ -i \frac{dA'_p(t)}{dt} &= \kappa_p B(t) A'_p(t). \end{aligned} \quad (A1)$$

We have written the Fourier-transformed version of the equation in the second line. The solution to this first-order differential equation is

$$A'_p(t) = A'_p(0) \exp[i\kappa_p \int_0^t B(t') dt']. \quad (A2)$$

The Fourier transform of the Bose function is

$$B(t) = \int_{-\infty}^{\infty} e^{i\omega t - \gamma|\omega|} B(\omega) d\omega = -i \frac{d}{dt} \ln \Gamma \left(\frac{\gamma+it}{\beta} \right) \Gamma \left(1 + \frac{\gamma-it}{\beta} \right). \quad (A3)$$

We have introduced the convergence factor γ in the definition of $B(t)$. Substituting (A.3) to (A.2) and Fourier-transforming back, the final result for $A_p(\omega)$ is (ignoring the overall constant)

$$A_p(\omega) = \cosh \left(\frac{\beta\omega}{2} \right) B^{-\kappa_p} \left(\frac{\gamma}{\beta}, 1 + \frac{\gamma}{\beta} \right) \int_{-\infty}^{\infty} \frac{dt}{2\pi} e^{-i\omega t} B^{\kappa_p} \left(\frac{1}{2} + \frac{\gamma+it}{\beta}, \frac{1}{2} + \frac{\gamma-it}{\beta} \right). \quad (A4)$$

In this form, the integrand is free of singularities, and one can take γ to be zero. The beta function $B(x, y)$ in front of the integral gives T^{κ_p} and up to a constant, the beta function inside the integral becomes $1/\cosh^{\kappa_p}(\pi t/\beta)$ and one can carry out the integration to yield the Eq. (4.12).

- ¹ D. Bohm and D. Pines, Phys. Rev. **92**, 609 (1953).
- ² D. Pines and P. Nozières, *The Theory of Quantum Liquids* (Benjamin, Reading, Mass., 1966).
- ³ S. Tomonaga, Prog. Theor. Phys. **5**, 544 (1950).
- ⁴ H. U. Everts and H. Schulz, Solid State Commun. **15**, 1413 (1974).
- ⁵ For a recent comprehensive review of the one-dimensional interacting liquids and references to the original literature on bosonization, see H. J. Schulz, 1994 Les Houches Lectures Notes (cond-mat/9503150); J. Voit, Rep. Prog. Phys. **58**, 977 (1995).
- ⁶ D. B. Chklovskii, B. I. Shklovskii, and L. I. Glazman, Phys. Rev. B **46**, 4026 (1992); C. W. J. Beenakker, Phys. Rev. Lett. **64**, 216 (1990); A. M. Chang, Solid State Commun. **74**, 871 (1990).
- ⁷ S. Conti and G. Vignale, Phys. Rev. B **54**, 14309 (1996).
- ⁸ J. H. Han and D. J. Thouless, Phys. Rev. B **55** 1926 (1997).
- ⁹ I. L. Aleiner and L. I. Glazman, Phys. Rev. Lett. **72**, 2935 (1994).
- ¹⁰ M. Franco, and L. Brey, Preprint/9702239.
- ¹¹ A. L. Efros, Solid State Commun. **65**, 1281 (1988); A. L. Efros, *ibid.*, **67**, 1019 (1988).
- ¹² J. H. Han, Ph. D. Thesis, University of Washington, 1997.
- ¹³ R. Courant and D. Hilbert, *Methods of Mathematical Physics* (Interscience Publishers, New York, 1962).
- ¹⁴ C. de C. Chamon and X. G. Wen, Phys. Rev. B **49**, 8227 (1994).
- ¹⁵ L. Brey, private communication.
- ¹⁶ L. Brey, Phys. Rev. B **50**, 11861 (1994); D. B. Chklovskii, Phys. Rev. B **51**, 9895 (1995).
- ¹⁷ G. D. Mahan, *Many-particle Physics* (Plenum Press, New York, 1981).
- ¹⁸ X. G. Wen, Phys. Rev. B **44**, 5708 (1991).
- ¹⁹ C. de C. Chamon and E. Fradkin, cond-mat/9612185.
- ²⁰ F. Milliken, C. Umbach, and R. Webb, Solid State Commun. **97**, 309 (1996).
- ²¹ X. G. Wen, Int. J. Mod. Phys. B **6**, 1711 (1992); C. L. Kane and M. P. A. Fisher, Phys. Rev. B **46**, 15233 (1992).
- ²² A. M. Chang, L. N. Pfeiffer, and K. W. West, Phys. Rev. Lett. **77**, 2538 (1996).

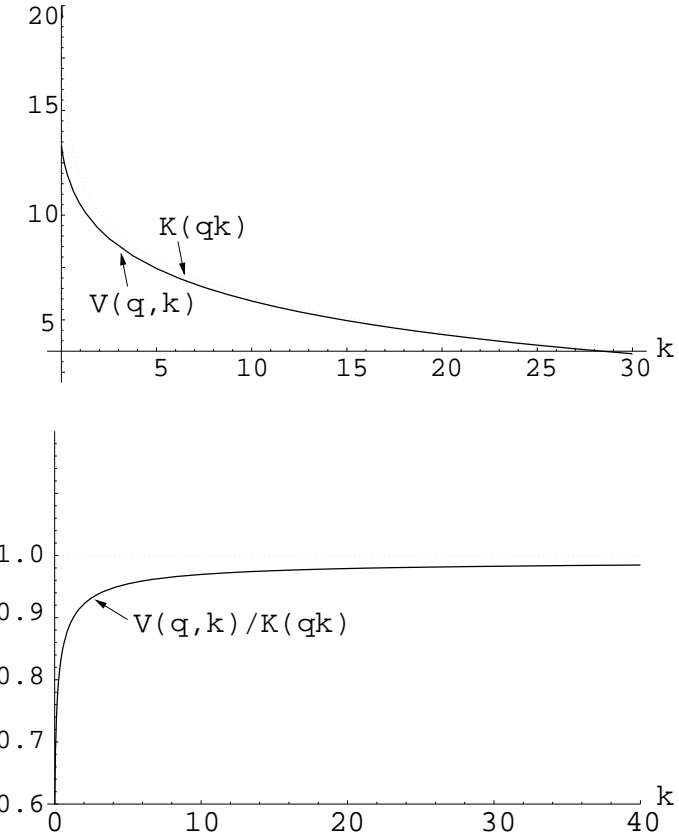


FIG. 1. Comparison of the classical kernel (denoted as $K(qk)$) and its quantum counterpart, $V(q,k)$, for $q = 10^{-2}$. For $qk \approx 0.3$ the two curves are already indistinguishable. In the bottom plot, the ratio $V(q,k)/K(qk)$ is shown. The classical kernel is always larger, but the difference quickly diminishes as k grows.

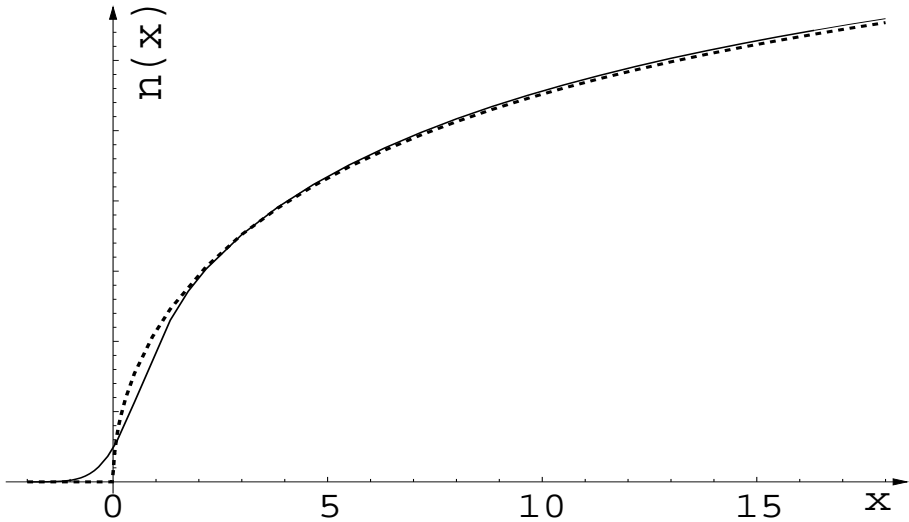


FIG. 2. Plot of the real space density $n(x) = \arctan(x/a)^{1/2}$ for $a = 10$ (dotted curve). The solid curve is the reconstructed plot according to Eq. (3.5) with $\Delta = 1$. The normalization A has been chosen to fit the asymptotic values of two curves. Except close to the edge, the difference is not very noticeable.

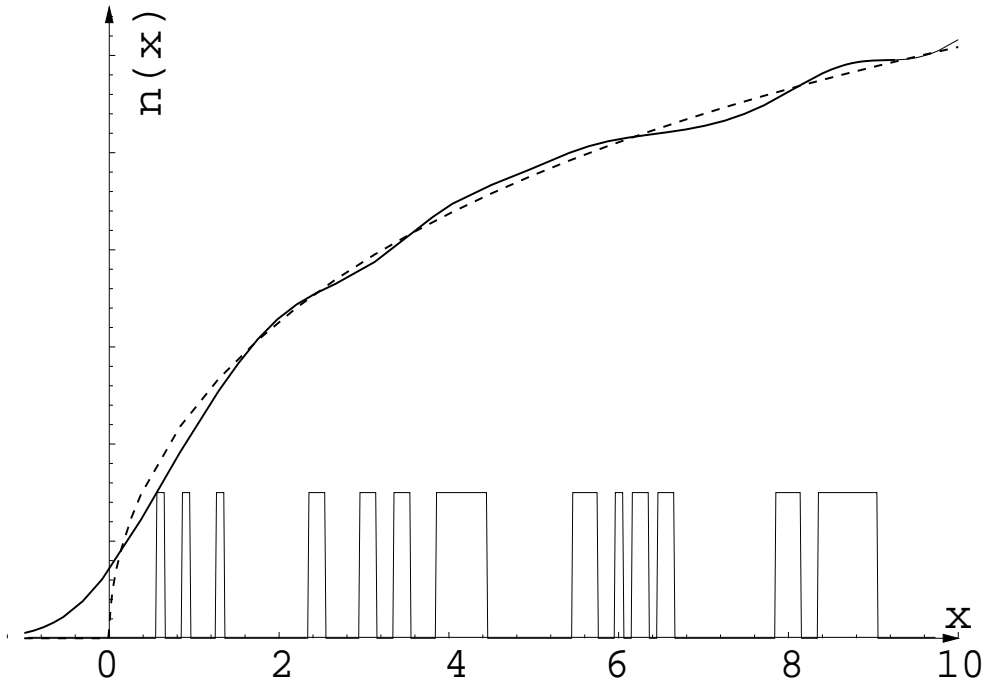


FIG. 3. The real space density constructed from the underlying islands of electrons (solid curve). Steps indicate filled states with $\delta x = 0.1$ as the width of a single state. Introducing a finer step width will smooth out fluctuations around the classical density (dotted curve) even more.